Supplementary Information

Internal Electric Fields in Asymmetric Single-layer Lattices for Enhancing Photocatalytic Solar-to-Hydrogen Efficiency

Yu-Liang Liu[a, b], Yongfeng Wan[a], Bo Li[a], Chuan-Lu Yang[b,*], Xingshuai Lv[c], Ying Shi[a,*]

[a] *Institute of Atomic and Molecular Physics, Jilin University, 130012 Changchun, China*

[b] *School of Physics and Optoelectronic Engineering, Ludong University, 26425 Yantai, China*

[c] *Institute of Applied Physics and Materials Engineering, University of Macau, Macao SAR 999078, China*

[*]*Corresponding author. Email:* shi_ying@jlu.edu.cn (Y. Shi); ycl@ldu.edu.cn (C.L. Yang)

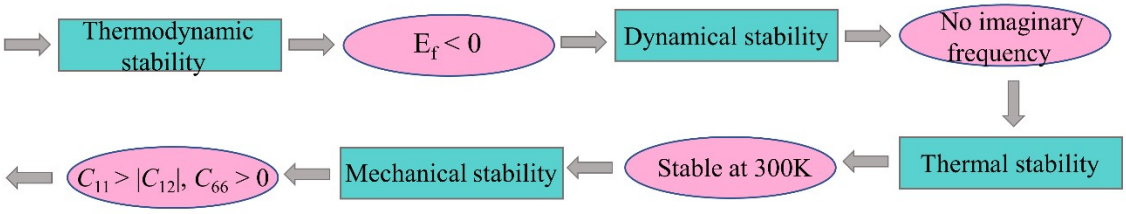

Fig. S1 The flow diagram of stability evaluation.

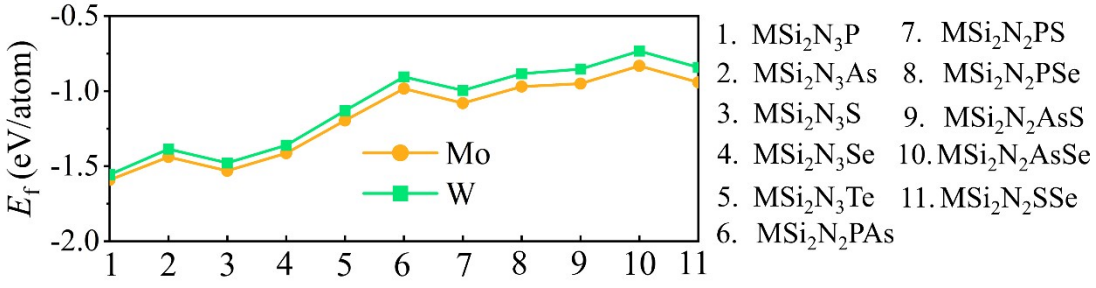

Fig. S2 The enthalpies of formation E_f (eV/atom) of 22 selected MSi_2N_2XY monolayers.

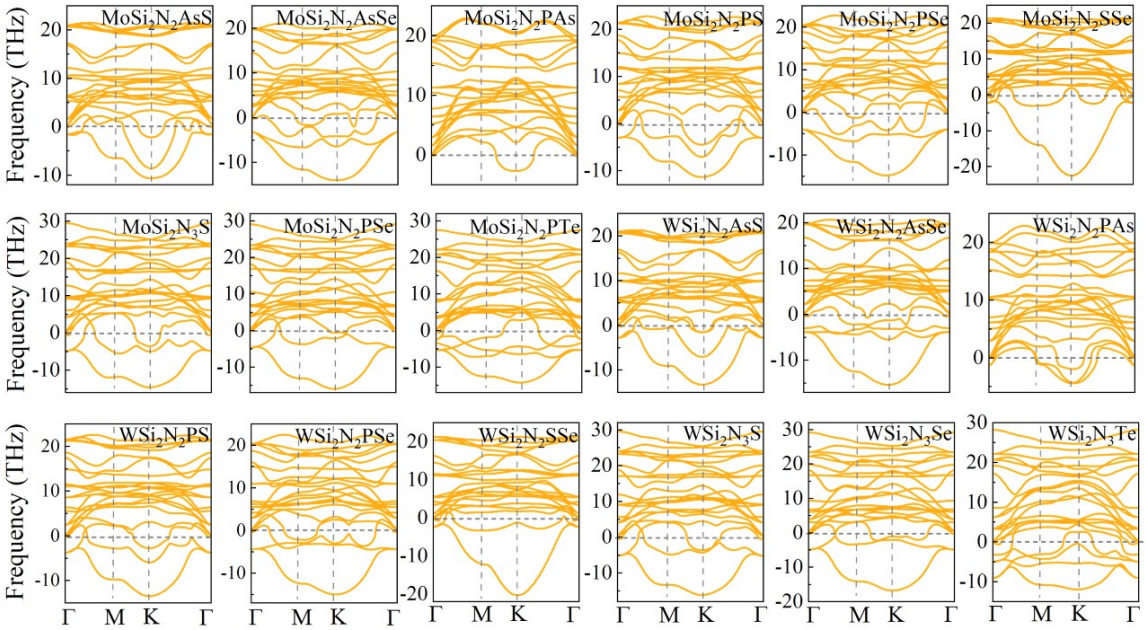

Fig. S3 The phonon spectrum of 18 unstable MSi_2N_2XY monolayers.

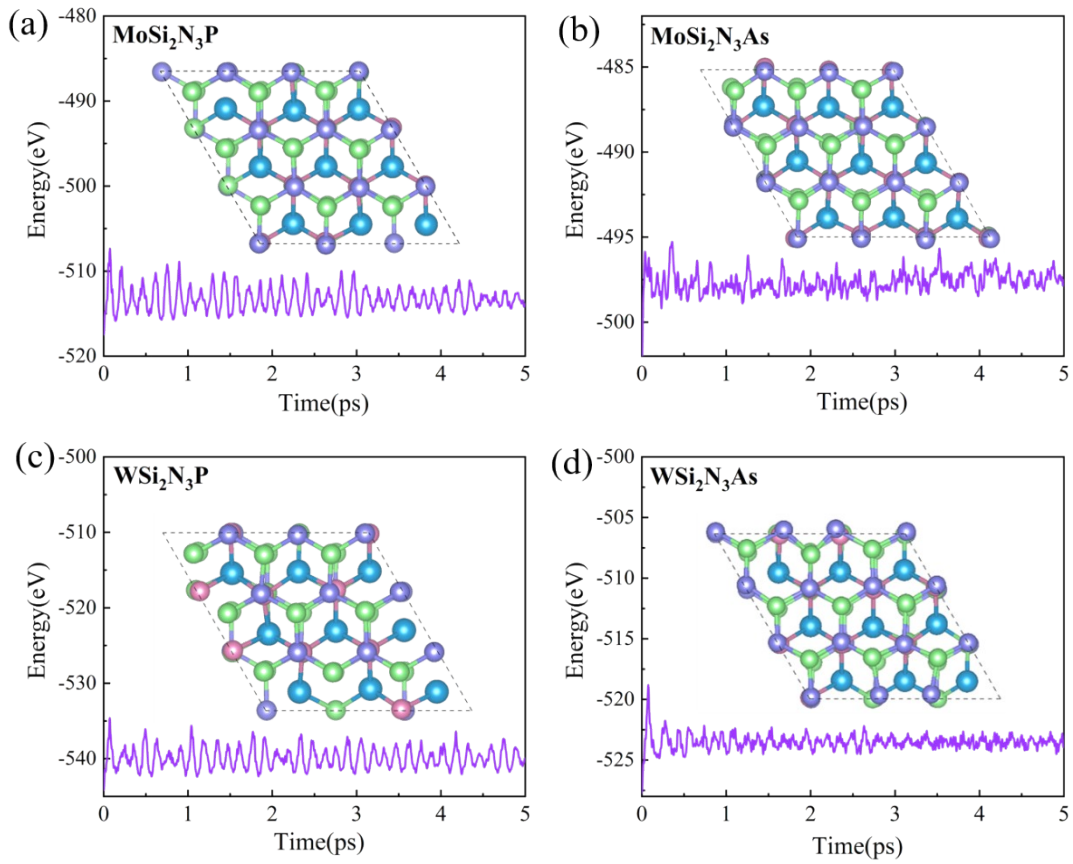

Fig. S4 The ab initio molecular dynamics (AIMD) simulations at 500 K for (a) $MoSi_2N_3P$, (b) $MoSi_2N_3As$, (c) WSi_2N_3P and (d) WSi_2N_3As monolayers, respectively.

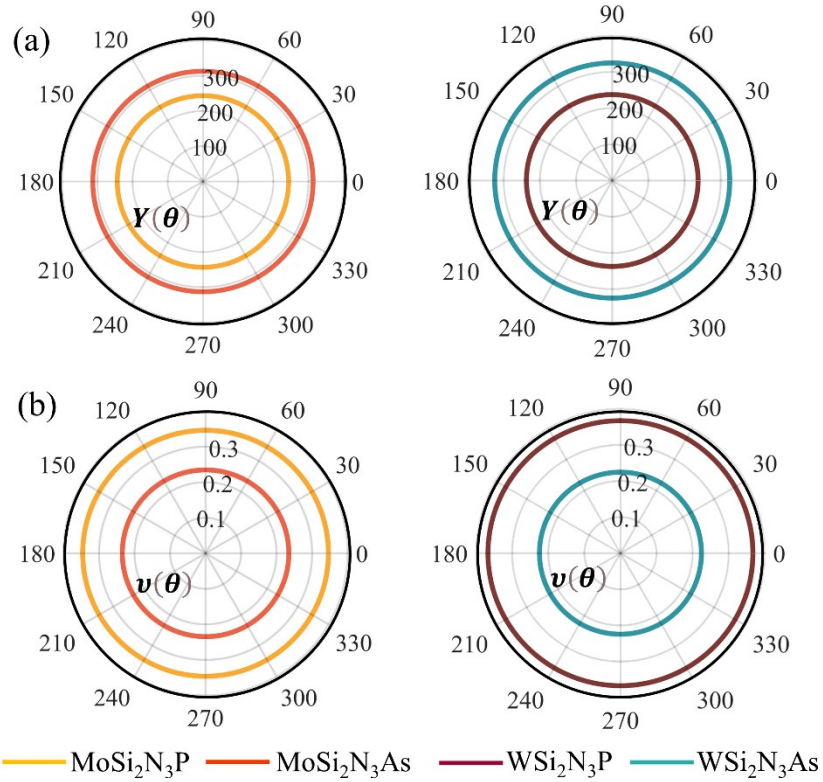

Fig. S5 Polar diagrams of (a) Young's modulus $Y(\theta)$ and (b) Poisson's ratio $\upsilon(\theta)$ for $MoSi_2N_3P$, $MoSi_2N_3As$, WSi_2N_3P and WSi_2N_3As monolayers.

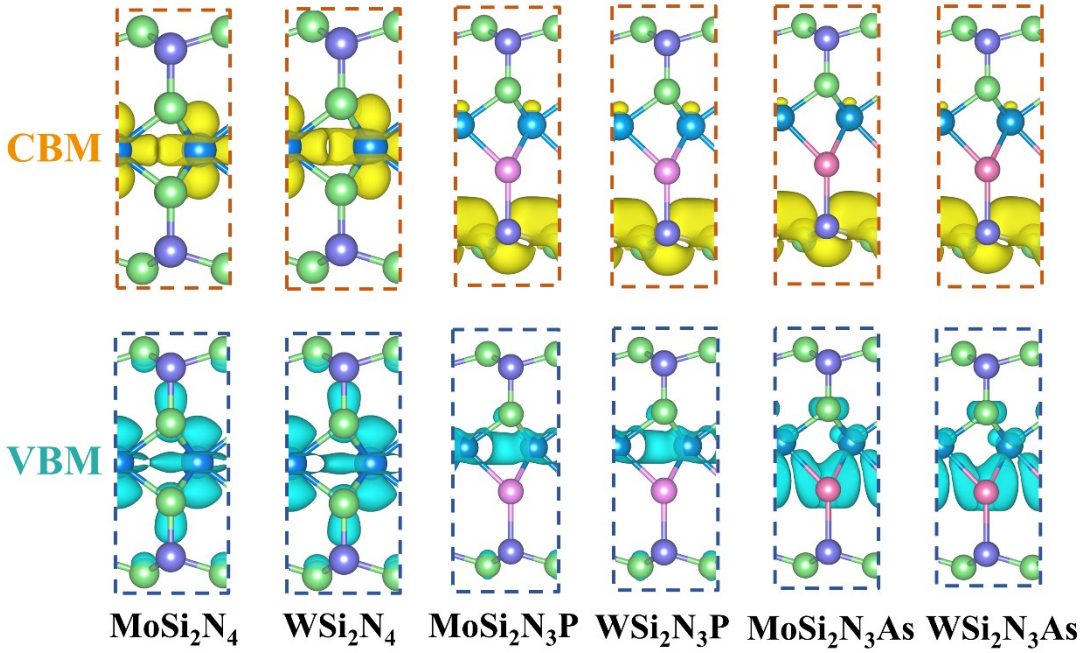

Fig. S6 Band-decomposed charge density of the CBM and VBM for MSi_2N_4, MSi_2N_3P and MSi_2N_3As monolayers, respectively.

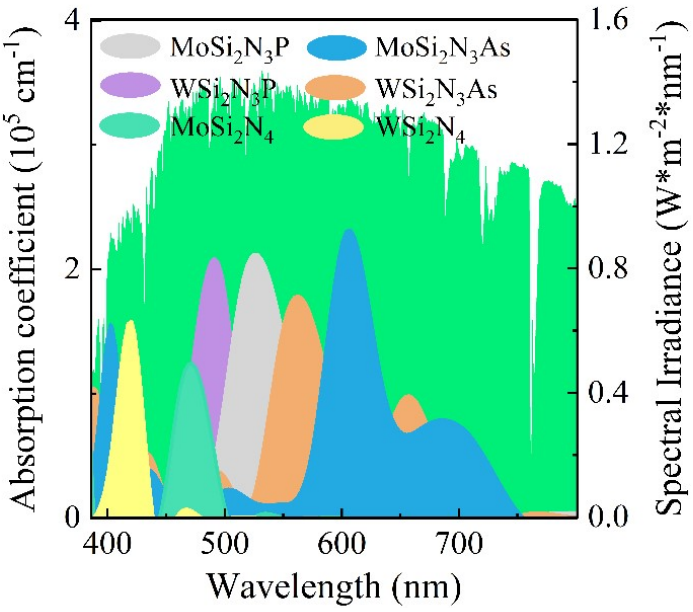

Fig. S7 The calculated absorption coefficients of MSi_2N_3Y monolayers and MSi_2N_4 monolayers by HSE06 functional.

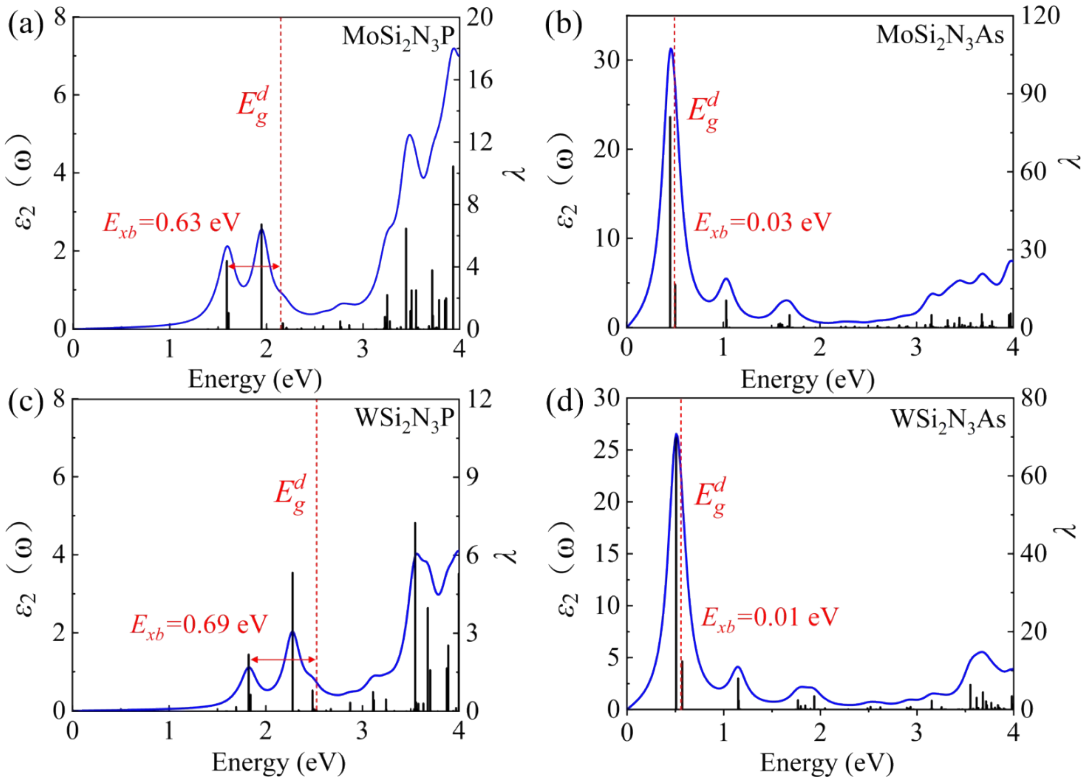

Fig. S8 (a)-(d) The imaginary dielectric function ε_2 and the oscillator strength λ as a function of photon energy for MSi_2N_3Y monolayers. The red line indicates the direct bandgap calcualted by GW mothod.

Table S1. The calculated structural properties, including lattice constant (a), bond length ($d^{out}_{Si-X/Y}$ and $d^{in}_{M-X/Y}$), and inner-layer height ($d^{in}_{Si-X/Y}$) for MSi_2N_2XY monolayers.

Monolayers	M	a (Å)	d^{out}_{Si-X} (Å)	d^{out}_{Si-Y} (Å)	d^{in}_{M-X} (Å)	d^{in}_{M-Y} (Å)	h^{in}_{X-Y} (Å)	Distortion (Y/N)
MSi_2N_4	Mo	2.901	1.751	1.751	2.087	2.087	2.490	N
	W	2.905	1.752	1.752	2.094	2.094	2.506	N
MSi_2N_3P	Mo	2.967	1.745	2.227	2.107	2.358	2.846	N
	W	2.974	1.746	2.222	2.117	2.367	2.868	N
MSi_2N_3As	Mo	2.982	1.746	2.337	2.106	2.463	2.973	N
	W	2.988	1.747	2.331	2.116	2.472	2.996	N
MSi_2N_3S	Mo	2.938	1.748	2.239	2.094	2.429	2.966	N
	W	2.937	1.748	2.269	2.102	2.432	2.986	N
MSi_2N_3Se	Mo	2.959	1.749	2.446	2.095	2.542	3.094	N
	W	2.959	1.747	2.516	2.103	2.540	3.106	N
MSi_2N_3Te	Mo	3.000	1.749	2.695	2.104	2.726	3.298	N
	W	3.003	1.749	2.735	2.114	2.737	3.327	N
MSi_2N_2PAs	Mo	3.051	2.230	2.353	2.363	2.488	3.333	N
	W	3.053	2.229	2.353	2.375	2.499	3.363	N
MSi_2N_2PS	Mo	3.007	2.248	2.200	2..363	2.448	3.329	N
	W	3.011	2.252	2.216	2.376	2.449	3.344	N
MSi_2N_2PSe	Mo	3.034	2.241	2.396	2.345	2.579	3.452	N
	W	3.040	2.245	2.424	2.361	2.584	3.475	N
MSi_2N_2PTe	Mo	3.072	2.237	3.854	2.351	2.751	3.646	Y
	W	3.091	2.236	3.881	2.366	2.736	3.628	Y
MSi_2N_2AsS	Mo	3.025	2.371	2.198	2.493	2.405	3.432	N
	W	3.032	2.375	2.218	2.501	2.418	3.453	N
MSi_2N_2AsSe	Mo	3.055	2.367	2.398	2.463	2.543	3.551	N
	W	3.059	2.370	2.432	2.476	2.552	3.578	N
MSi_2N_2AsTe	Mo	3.092	2.363	3.871	2.460	2.723	3.749	Y
	W	3.028	2.379	2.760	2.452	3.150	4.339	Y
MSi_2N_2SSe	Mo	3.023	2.217	2.440	2.327	2.637	3.515	N
	W	3.021	2.237	2.485	2.355	2.619	3.536	N
MSi_2N_2STe	Mo	3.072	2.199	3.743	2.348	2.776	3.675	Y
	W	3.075	2.218	3.735	2.372	2.768	3.697	Y
MSi_2N_2SeTe	Mo	3.098	2.387	3.619	2.490	2.719	3.780	Y
	W	3.100	2.412	3.799	2.515	2.729	3.826	Y

For a mechanically stable material, the elastic constants should fulfill the Born-Huang stability criteria[1]: $C_{11} > |C_{12}|$, $C_{11}C_{22} - {C_{12}}^2 > 0$, $C_{66} > 0$. Considering that Janus $MoSi_2N_3P$ belongs to C_{3v} point group, thus $C_{11} = C_{22}$ and $C_{66} = 0.5(C_{11} - C_{12})$, the criterion turns out to be only $C_{11} > |C_{12}|$. As shown in Table S3, the calculated C_{11} is larger than C_{12} suggesting that four $MoSi_2N_3Y$ monolayers are mechanically stable. To evaluate the in-plane stiffness, we calculated Young's modulus $Y(\theta)$ and Poisson's ratio $\upsilon(\theta)$ along the in-plane θ, which is given as follow:

$$Y(\theta) = \frac{C_{11}C_{22} - {C_{12}}^2}{C_{11}\,sin^4\theta + A\,sin^2\theta\,cos^2\theta + C_{22}\,cos^4\theta} \quad (1)$$

$$\upsilon(\theta) = \frac{C_{12}\,sin^4\theta - B\,sin^2\theta\,cos^2\theta + C_{12}\,cos^4\theta}{C_{11}\,sin^4\theta + A\,sin^2\theta\,cos^2\theta + C_{22}\,cos^4\theta} \quad (2)$$

where $A = \left(C_{11}C_{22} - {C_{12}}^2\right)/C_{66} - 2C_{12}$ and $B = C_{11} + C_{22} - \left(C_{11}C_{22} - {C_{12}}^2\right)/C_{66}$.

Table S2. The obtained in-plane elastic constants C_{11}, C_{22}, C_{12} and C_{66} of four monolayers.

Monolayers	C_{11} (N/m)	C_{22} (N/m)	C_{12} (N/m)	C_{66} (N/m)
$MoSi_2N_3P$	331.0	331.0	77.6	126.7
$MoSi_2N_3As$	276.4	276.4	95.6	90.4
WSi_2N_3P	341.8	341.8	76.7	132.5
WSi_2N_3As	274.1	274.1	100.6	86.8

Table S3. The calculated band gap at HSE06 level (E_g), the potentials of photo-generated electrons/holes (U_e/U_h), dipole moments (μ) and electrostatic potential difference ($\Delta\Phi$) for four stable monolayers.

Monolayers	E_g (eV)	U_e (eV)	U_h (eV)	μ (Debye)	$\Delta\Phi$ (eV)

$MoSi_2N_3P$	0.96	1.37	1.71	0.43	2.12
$MoSi_2N_3As$	0.46	1.36	1.65	0.53	2.55
WSi_2N_3P	0.79	1.37	1.42	0.40	2.00
WSi_2N_3As	0.45	1.37	1.54	0.48	2.46

The Gibbs free energy

The change of Gibbs free energy (ΔG) in water splitting reaction is calculated using the method proposed by Nørskovet *et al*[2]. The formula can be expressed as:

$$\Delta G = \Delta E + \Delta E_{ZPE} - T\Delta S \tag{3}$$

where ΔE is the adsorption energy, ΔE_{ZPE} and ΔS are the differences in the zero-point energy and entropy difference between the adsorbed state and corresponding free-standing state, respectively.

E_{ZPE} could be derived after the frequency calculation by

$$E_{ZPE} = {}^{1}/_{2}\sum h\nu \tag{4}$$

where ν represents the vibrational frequency.

Meanwhile, TS is given by

$$TS = k_b T\left[\sum_K \ln\left(\frac{1}{1 - e^{-h\nu/k_b T}}\right) + \sum_K \frac{h\nu}{k_b T}\left(\frac{1}{e^{-h\nu/k_b T} - 1} + 1\right)\right] \tag{5}$$

where *e* represents the electron charge, *h* represents Planck's constant and k_b is Boltzmann's constant. Here, T is set to be 298.15K.

The effect of external potential and pH have been taken into account to evaluate the HER and OER activities. The ΔG for HER process include two steps, which was expressed as:

$$(1)\quad * + H^+ + e^- \rightarrow H^* \tag{6}$$

$$\Delta G_1 = G_{H^*} - \frac{1}{2}G_{H_2} - G_* + \Delta G_U + \Delta G_{pH}$$
$$= \Delta E_H + \Delta E_{ZPE(H)} - T\Delta S_H + \Delta G_U + \Delta G_{pH}$$

$= \Delta G_H$ (7)

(2) $H^* + H^+ + e^- \rightarrow * + H_2(g)$ (8)

$$\Delta G_2 = G_* + \frac{1}{2}G_{H_2} - G_{H^*} + \Delta G_U + \Delta G_{pH}$$
$$= -(\Delta E_H + \Delta E_{ZPE(H)} - T\Delta S_H) + \Delta G_U + \Delta G_{pH}$$
$$= -\Delta G_H + 2\Delta G_U + 2\Delta G_{pH} \quad (9)$$

Meanwhile, the OER can be decomposed into four elementary steps. The ΔG for each step was calculated as follows:

(3) $H_2O(l) + * \rightarrow OH^* + H^+ + e^-$

(10)

$$\Delta G_3 = G_{OH^*} + \frac{1}{2}G_{H_2} - G_* - G_{H_2O} + \Delta G_U - \Delta G_{pH}$$
$$= \Delta E_{OH} + \Delta E_{ZPE(OH)} - T\Delta S_{OH} + \Delta G_U - \Delta G_{pH}$$
$$= \Delta G_{OH} \quad (11)$$

(4) $OH^* \rightarrow O^* + H^+ + e^-$

(12)

$$\Delta G_4 = G_{O^*} + \frac{1}{2}G_{H_2} - G_{OH^*} + \Delta G_U - \Delta G_{pH}$$
$$= (\Delta E_O + \Delta E_{ZPE(O)} - T\Delta S_O + 2\Delta G_U - 2\Delta G_{pH}) - (\Delta E_{OH} + \Delta E_{ZPE(OH)} - T\Delta S_{OH} + G_U - \Delta G_{pH})$$

$$= \Delta G_O - \Delta G_{OH} \quad (13)$$

(5) $H_2O(l) + O^* \rightarrow OOH^* + H^+ + e^-$

(14)

$$\Delta G_5 = G_{OOH^*} + \frac{1}{2}G_{H_2} - G_{O^*} - G_{H_2O} + \Delta G_U - \Delta G_{pH}$$
$$= (\Delta E_{OOH} + \Delta E_{ZPE(OOH)} - T\Delta S_{OOH} + 3\Delta G_U - 3\Delta G_{pH}) - (\Delta E_O + \Delta E_{ZPE(O)} - 2\Delta G_U - 2\Delta G_{pH})$$

$$= \Delta G_{OOH} - \Delta G_O \quad (15)$$

$$OOH^* \rightarrow * + O_2(g) + H^+ + e^- \quad (6)$$

(16)

$$\Delta G_6 = G_* + \frac{1}{2}G_{H_2} + G_{O_2} - G_{OOH^*} + \Delta G_U - \Delta G_{pH}$$
$$= (4.92 + 4\Delta G_U - 4\Delta G_{pH}) - (\Delta E_{OOH} + \Delta E_{ZPE(OOH)} - T\Delta S_{OOH} + 3\Delta G_U - 3\Delta G_{pH})$$
$$= (4.92 + 4\Delta G_U - 4\Delta G_{pH}) - \Delta G_{OOH} \quad (17)$$

where ΔG_U ($\Delta G_U = -eU$) denotes extra potential bias provided by an electron in the electrode, where U represents the potential difference from the standard hydrogen electrode potential. ΔG_{pH} represents the effect of pH on ΔG, which is calculated by $\Delta G_{pH} = k_b T \times ln10 \times$ pH.

Table S4. The adsorption energies ΔE (eV) of all adsorbed species on four structures.

Species	$MoSi_2N_3P$	$MoSi_2N_3As$	WSi_2N_3P	WSi_2N_3As
H^*	-0.15	-0.84	-0.16	-0.80
OH^*	0.86	0.71	0.80	0.63
O^*	3.40	3.17	3.30	2.75
OOH^*	4.30	4.14	4.23	4.06

Table S5. The zero-point energy E_{ZPE} (eV) and entropy TS (eV) of molecules and adsorbates on four structures.

Species	$MoSi_2N_3P$	$MoSi_2N_3As$	WSi_2N_3P	WSi_2N_3As
H_2O(l)	0.56/0.67	0.56/0.67	0.56/0.67	0.56/0.67
H_2(g)	0.27/0.41	0.27/0.41	0.27/0.41	0.27/0.41
H^*	0.24/0.01	0.23/0.01	0.24/0.01	0.23/0.01
OH^*	0.37/0.09	0.37/0.09	0.38/0.09	0.37/0.09
O^*	0.07/0.06	0.07/0.06	0.07/0.06	0.08/0.06
OOH^*	0.46/0.17	0.46/0.17	0.45/0.18	0.46/0.16

Carrier mobility

The carrier mobility of MSi_2N_3Y monolayers are calcualted based on the deformation potential (DP) approach [3], which is expressed by the following equation:

$$\mu = \frac{2e\hbar^3 C}{3k_B T|m^*|^2 {E_d}^2} \quad \text{(S18)}$$

where e, $\hbar$ and k_B are electron charge, the reduced Planck constant and Boltzmann constant, T means the temperature. C and E_d represent the elastic modulus and deformation potential constant. C can be obtained from $C = \frac{1}{S_0}\frac{\partial^2 E}{\partial \varepsilon^2}$, where E_d is the total energy of the system under uniaxial strain, S_0 is the area of the system, and ε is

the ratio of lattice parameter under the uniaxial strain along *x* or *y* direction on the rectangle cell and. E_d is represented by $E_d = \frac{\partial E_{edge}}{\partial \varepsilon}$, and E_{edge} is the energy change of band edge under uniaxial strain. At the meantime, the effective mass *m** is calculated from the following relations:

$$\frac{1}{m^*} = \frac{1}{\hbar^2}\frac{d^2E(k)}{dk^2} \quad \text{(S19)}$$

where *k* is wave vector and *E(k)* represents the energy that corresponding to *k*.

Solar-to-hydrogen (STH) efficiency

STH efficiency is estimated by the product of the efficiency of light absorption η_{abs} and carrier utilization η_{cu} using the following expression[4]:

$$\eta_{STH} = \eta_{abs} \times \eta_{cu} \quad (20)$$

The efficiency of light absorption is defined as:

$$\eta_{abs} = \frac{\int_{E_g}^{\infty} P(\hbar\omega)d(\hbar\omega)}{\int_{0}^{\infty} P(\hbar\omega)d(\hbar\omega)} \quad (21)$$

where E_g is the band gap of photocatalyst and $P(\hbar\omega)$ is the AM1.5 solar energy flux at the photon energy $\hbar\omega$.

The efficiency of carrier utilization (η_{cu}) is estimated by

$$\eta_{cu} = \frac{\Delta G_{H_2O}\int_{E}^{\infty}\frac{P(\hbar\omega)}{\hbar\omega}d(\hbar\omega)}{\int_{E_g}^{\infty} P(\hbar\omega)d(\hbar\omega)} \quad (22)$$

where ΔG_{H_2O} is the potential difference for water splitting (1.23 eV) and E is the energy of photons that can be used for water splitting, which can be defined as

$$E=\begin{cases} E_g, (\chi(H_2)\geq 0.2, \chi(O_2)\geq 0.6) \\ E_g+0.2-\chi(H_2), (\chi(H_2)<0.2, \chi(O_2)\geq 0.6) \\ E_g+0.6-\chi(O_2), (\chi(H_2)\geq 0.2, \chi(O_2)<0.6) \\ E_g+0.8-\chi(H_2)-\chi(O_2), (\chi(H_2)<0.2, \chi(O_2)<0.6) \end{cases} \quad (23)$$

where $\chi(H_2)$ and $\chi(O_2)$ are the over potentials for HER and OER, respectively. Considering the energy loss during carrier migration between different materials, the required over potentials for HER and OER are assumed to be 0.2 and 0.6 eV, respectively.

The intrinsic electric filed does positive work for the electron-hole separation during the process of photocatalytic water splitting. Therefore, this part of work should be added into the total energy, and then the corrected STH efficiency of photocatalytic water splitting for 2D material with vertical intrinsic EF is calculated as

$$\eta'_{STH}=\eta_{STH}\times\frac{\int_0^{\infty}P(\hbar\omega)d(\hbar\omega)}{\Delta\Phi\int_{E_g}^{\infty}\frac{P(\hbar\omega)}{\hbar\omega}d(\hbar\omega)+\int_0^{\infty}P(\hbar\omega)d(\hbar\omega)} \quad (24)$$

where $\Delta\Phi$ is the vacuum level difference on the two respective surfaces.

Table S6. The calculated Over-Potential for HER $\chi(H_2)$, Over-Potential for OER $\chi(O_2)$, the photons energy (E), energy conversion efficiency of light absorption (η_{abs}), carrier utilization (η_{cu}), and corrected STH (η'_{STH}) of four monolayers pH=7.

Monolayers	$\chi(H_2)$ (eV)	$\chi(O_2)$ (eV)	E (eV)	η_{abs} (%)	η_{cu} (%)	η'_{STH} (%)
$MoSi_2N_3P$	0.96	0.89	0.96	91.13	70.89	30.57
$MoSi_2N_3As$	0.95	0.82	0.46	99.82	78.41	29.84
WSi_2N_3P	0.96	0.60	0.79	95.52	74.20	32.93
WSi_2N_3As	0.97	0.72	0.45	99.82	78.41	30.51

References

1. R. C. Andrew, R. E. Mapasha, A. M. Ukpong, N. Chetty, *Phy. Rev. B* 2012**,** 85, 125428.
2. J. K. Nørskov, J. Rossmeisl, A. Logadottir, L. Lindqvist, J. R. Kitchin, T. Bligaard, H. Jónsson, *J. Phy. Chem. B* 2004**,** 108, 17886.
3. J. Bardeen, W. Shockley, *Phys. Rev.* 1950, 80, 72-80.
4. C.F. Fu, J. Sun, Q. Luo, X. Li, W. Hu, J. Yang, *Nano Lett.* 2018**,** 18, 6312-6317.